ELSEVIER

Journal of Photochemistry and Photobiology A: Chemistry 114 (1998) 109–116

Journal of Photochemistry and Photobiology A:Chemistry

Minimum energy paths in the excited and ground states of short protonated Schiff bases and of the analogous polyenes

Marco Garavelli [a], Fernando Bernardi [a,*], Paolo Celani [b], Michael A. Robb [b], Massimo Olivucci [a]

[a] *Dipartimento di Chimica 'G. Ciamician', Università di Bologna via Selmi n. 2, Bologna I-40126, Italy*

[b] *Department of Chemistry, King's College London Strand, London WC2R 2LS, UK*

Received 30 June 1997; accepted 16 October 1997

Abstract

A theoretical study of the minimum energy paths (MEP) for the first excited state S_1 and for the ground state S_0 of two short-chain protonated Schiff bases (the protonated *s-cis* 1-iminium-2-propene $H_2C{=}CH{-}CH{=}NH_2+$ and the protonated *tZt* 1-iminium-2,4-pentadiene $H_2C{=}CH{-}CH{=}CH{-}CH{=}NH_2+$) and of the two analogous polyenes (*s-cis* butadiene $H_2C{=}CH{-}CH{=}CH_2$ and *tZt* hexatriene $H_2C{=}CH{-}CH{=}CH{-}CH{=}CH_2$) is reported. The geometries have been optimized at the CAS-SCF level and the energetics have been refined via single-point computations at the multi-reference MP2 level. It is demonstrated that the photochemistry of the protonated Schiff bases and of the analogous polyenes is driven by two different S_1 excited states, the spectroscopic 1B ionic state for the protonated Schiff bases and the covalent $2A_1$ excited state for the analogous polyenes. This difference induces different electronic and geometric features in the computed MEP and conical intersections which depend on the nature of the involved excited states. The conical intersections between S_1/S_0 in polyenes have a covalent tetraradicaloid nature and are characterized by the development of a typical $(-CH-)_3$ 'kink' in the carbon moiety, while the conical intersection points in the protonated Schiff bases have a twisted double bond. Thus in the protonated Schiff bases, the photoproducts arise only from isomerization processes, while in the analogous polyenes, the photoproducts arise from various types of recoupling schemes of the electrons of the quasi-tetraradical conical intersection point, leading to a more complex photoreactivity pattern.

Keywords: Minimum energy paths; Schiff bases; Analogous polyenes

1. Introduction

The photophysics and photochemistry of protonated Schiff bases (PSB) is the subject of current experimental [1–10] and theoretical [11–22] work. Interest in this class of compounds is motivated by the fact that a widespread family of photoreceptors, the rhodopsin proteins [1,2], contain a retinal chromophore bound to the protein via a Schiff base linkage (usually to the amino acid lysine). It is now accepted that the protein is active only if the Schiff base nitrogen is protonated and thus forms a polyeniminium cation (see Eq. (1)).

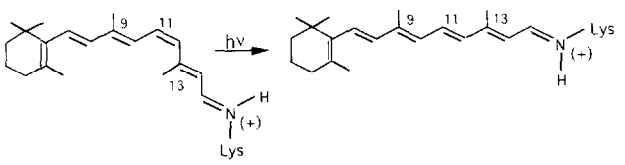

(1)

The photoinduced *cis–trans* isomerization of the PSB chromophore triggers the conformational changes underlying the protein biological functions such as the initial steps in the process of vision [1] and in the process of photosynthesis in halobacteria [2]. However, the detailed nature of the potential energy surface corresponding to the lowest energy excited states in PSB remains an outstanding and important problem. PSB cations and polyenic hydrocarbons are isoelectronic. The only structural difference between a linear PSB and its polyenic analogue is the replacement of the terminal $=NH_2+$ group with a $=CH_2$ group. Since the protonation of the imine group eliminates the low-lying $n-\pi^*$ states in Schiff bases, polyenes and PSB have a similar set of excited states which are derived from the excitation of the π-system alone. Because of these similarities, polyenes have been often considered good experimental and theoretical models for understanding the excited state behaviour and photochemical reactivity of retinal chromophores. In this paper we report a systematic exploration of the excited state relaxation and reaction pathways of PSB starting at the vertical excitation

* Corresponding author.

1010-6030/98/$19.00
PII S1010-6030(98)00218-4

region. Two short linear PSB have been studied: the *s-cis* 1-iminium-2-propene cation (*s-cis* $H_2C{=}CH{-}CH{=}NH_2+$, denoted here as PSB1) and the *tZt* 1-iminium-2,4-pentadiene cation (*tZt* $H_2C{=}CH{-}CH{=}CH{-}CH{=}NH_2+$, denoted here as PSB2). The computed relaxation paths are compared with those of the isoelectronic polyenes *s-cis* buta-1,3-diene ($H_2C{=}CH{-}CH{=}CH_2$ denoted here as *s-cis* butadiene) and *tZt* hexa-1,3,5-triene (*tZt* $H_2C{=}CH{-}CH{=}CH{-}CH{=}CH_2$ denoted here as *tZt* hexatriene) (see Scheme 1).

In polyenes the lowest *relaxed* (i.e., non vertical) excited state does not correspond to the spectroscopic state but rather to the doubly excited $2A_1$ (covalent) excited state. (In this work, we use symmetry labels 1B and 2A to refer to the ionic and excited covalent states of the two studied short-chain PSB and symmetry labels $1B_2$ and $2A_1$ for the corresponding ionic and covalent states of the two analogous polyenes). In contrast, recent computational studies of retinal-like PSB have provided evidence that the lowest excited state in PSB is the ionic allowed 1B state and thus the analogous polyenes may not be good models for PSB photophysics and chemistry as previously supposed.

Du and Davidson [11], using MRSD-CI computations, suggested that the lowest vertically excited state in PSB11 (the 11-*cis* isomer of the PSB of retinal) is the spectroscopically allowed 1B state. They also investigated the methaniminium ($CH_2{=}NH_2+$) and 1-iminium-2-propene ($H_2C{=}CH{-}CH{=}NH_2+$) cations [12] and the spectroscopic 1B state was found to correspond to the first excited state. Martin [13,14] has computed, using a semi-empirical effective Hamiltonian technique, the vertical excitation energies for a series of all-*trans* PSB going from the methaniminium to the 1-iminium-2,4,6,8,10-pentene cation. His results show that, unlike polyenes, where the 2A and 1B energies are very close in the vertical region, in PSB, the 2A vertical excitation energy is considerably larger than that of the spectroscopic state. Martin [13,14] finds a 2A–1B gap of 43 kcal/mol for $H_2C{=}CH{-}CH{=}NH_2+$ and 31 kcal/mol for $H_2C{=}CH{-}CH{=}CH{-}CH{=}NH_2+$ and Du and Davidson [11] report a gap of 37 kcal/mol for the 1-iminium-2,4,6,8,10-pentene cation.

Investigations of the excited state energetics of short PSB cations along *assumed* isomerization coordinates (i.e., the dihedral angle of rotation around the isomerizing double bond) have been carried out by Bonacic-Koutecky et al. [15,16] and, more recently, by Dobado and Nonella [17] using ab initio MRD-CI and MRSD-CI computations, respectively. For the 1-iminium-2-propene cation, Bonacic-Koutecky et al. [16] found that the singly excited 1B state was the lowest excited state along the assumed reaction coordinate. Nonella et al. investigated the structure of the first excited state and S_0 potential energy surfaces along two adjacent torsions (about the C_β–C_γ and C_α–C_β bonds) for the all-*trans* 1-iminium-2-4-pentadiene cation (*tEt* C_5H_6-NH_2+). Such computations appear to agree with the results of earlier semi-empirical studies by Dormans et al. [18], where it was found that the ionic 1B state is the lowest excited state along an assumed reaction coordinate.

The vertical excitation region of polyenes is also well documented. Roos et al., using the CAS-PT2 method [23,24], have computed the vertical excitation energies of a series of unsaturated hydrocarbons including *s-cis* butadiene and *tZt* hexatriene [25]. Like PSB, the spectroscopic 1B states in polyenes correspond to the first excited state; however, the energy gap between the spectroscopic and dark 2A excited state is much smaller than in the related PSB: about 12 kcal/mol in *s-cis* butadiene and only 1 kcal/mol in *tZt* hexatriene. Recently, we have published an account of the structure of the potential energy surface and relaxation pathway for *s-cis* butadiene [26] where we show that the initially prepared $1B_2$ state of the molecule relaxes very rapidly to the $2A_1$ state via a $1B_2/2A_1$ surface crossing. After the decay, the molecule evolves along the $2A_1$ state. The computed $2A_1$ minimum energy path (MEP) rationalizes the observed photochemistry of this molecule (including double-bond *cis–trans* isomerization and rearrangements). The $2A_1$ reaction path terminates at a $2A_1/S_0$ conical intersection which provides a fully efficient radiationless decay channel to the ground state leading to photoproduct formation.

The S_1/S_0 conical intersection found in *s-cis* butadiene [27] and other polyenes (including hexatrienes [28] and octatetraene [29]) suggests that the existence, structure and accessibility of conical intersections in PSB may also control the photophysics and photochemistry in these molecules. Weiss and Warshel [19] and Warshel and Barboy [20] were the first to suggest that an *unusually large* decay probability, which prevents excited state equilibration, is required to explain the observed high quantum yield and short reaction time in rhodopsin photoisomerization. These suggestions have been supported by the experimental work of Schoenlein et al. [3] and Wang et al. [4] who suggested that the extremely fast isomerization of PSB11 in rhodopsin can be explained by a Landau–Zener dynamical internal conversion process [30,31]. The presence of a conical intersection [32] (i.e., a real crossing) between the S_1 and S_0 potential energy surfaces of PSB11 and located at the end of a S_1 relaxation path would provide a clear-cut explanation of the extreme velocity of such radiationless decay. The involvement of a conical intersection in the photoisomerization of PSB11 has

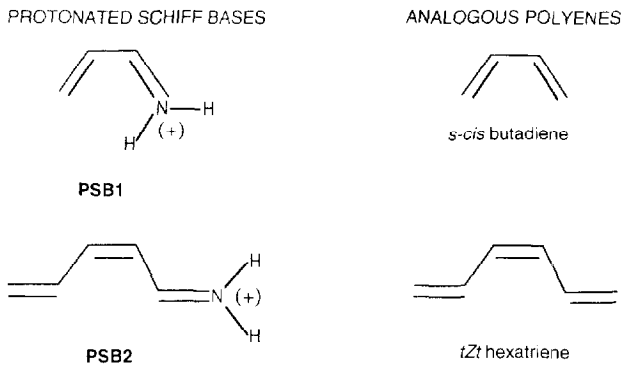

Scheme 1.

been suggested before [15,16], and recently [33] we have shown direct computational evidence of such feature for a minimal triene model (PSB2).

In this paper, we report the results of a comparative study of the MEP computed for the short-chain PSB, PSB1 and PSB2, and for the two analogous polyenes (see Scheme 1), where the structures of all stationary points and MEP have been optimized at the CAS-SCF level [34,35] and the energetics refined via single-point computations at the multi-reference MP2 level [36,37]. It is shown that the excited state evolution of the two PSB and of the analogous polyenes is driven by electronically different S_1 excited states, the spectroscopic 1B ionic state for the PSB and the covalent $2A_1$ excited state for the analogous polyenes. *Thus, we conclude that polyenes are not suitable models for the investigation of the retinal chromophore or other PSB photochemistry*. Furthermore, the different nature of the electronic states in this class of compounds induces *different* electronic and geometric features in the computed S_1 MEP and in the structure of the $S_1 \rightarrow S_0$ decay channel. In particular we show that, while the decay channel in polyenes has a covalent 'quasi-tetraradicaloid' nature [29], the S_1/S_0 conical intersection points found in PSB have a twisted double-bond (the central double bond for PSB2 and the CH_2=CH– double bond for PSB1) and correspond to a type of twisted intramolecular charge transfer (TICT) states [38]. Consequently, while in the PSB the only predicted photoproducts correspond to *cis–trans* isomers, in polyenes we also expect rearrangement products arising from different types of recoupling of the 'quasi-tetraradicaloid' unpaired electrons.

2. Computational details

The structures of all the stationary points and MEP discussed in this paper have been optimized at the CAS-SCF level of theory [34] using the methods available in the Gaussian 94 package of programs [35]. To take into account the effect of dynamic electron correlation, the energetics of the CAS-SCF (excited and ground state) optimized structures have been refined via single-point computations at the multi-reference Møller–Plesset perturbation level of theory using the PT2F method [36] included in MOLCAS-3 [37].

For the two short PSB investigated in this work, MC-SCF energy and gradient computations have been carried out using a complete active space (CAS) with the 6-31 + G* basis set available in Gaussian 94 [35]. The S_0 minima and the S_0 MEP have been computed using a 4 electron/4 π orbital CAS for PSB1 and a 6 electron/6 π orbital CAS for PSB2. The S_1 MEP and the S_1 no-planar points have been computed using state average orbitals. To correct for the loss in accuracy due to the use of state average orbitals, we have used an augmented 4 electron/10 π orbital CAS for PSB1 and 6 electron/9 π orbital CAS for PSB2 (in order to limit the cost of such computations we have used the 6-31G* basis set for S_1 MEP computations in the case of the longer PSB, since geometry optimizations on S_1 PSB2 and PSB1 has demonstrated that the two basis sets yield the same geometrical parameters). In order to improve the energetics by including the effect of dynamic electron correlation, the MC-SCF/6-31 + G* energies have been re-computed at the multi-reference Møller–Plesset perturbation level of theory using the PT2F method [36] with an augmented 4 electron/10 π orbital CAS for PSB1 and a 6 electron/12 π orbital CAS for PSB2 (see Ref. [33] for more details on PSB2 computations). For PSB, the CAS-PT2/6-31 + G* vertical excitation energies are in good agreement with other computational results available in literature [11–14]. Thus, we believe this level of accuracy is adequate for the purposes outlined in Section 1 of this paper.

In the case of the two polyenes, the S_0 critical points and MEP have been optimized using a 4 electron/4 π orbital CAS for *s-cis* butadiene and a 6 electron/6 π orbitals CAS for *tZt* hexatriene using the 6-31G* basis set. Excited states MEP and critical points have been optimized using the same active spaces and the DZ + d (Dunning–Huzinaga double-ζ + d-type polarization function) basis set.[1] The energetics on the $1B_2$ surface of butadiene have been computed at the CAS-PT2 level using a DZ + spd basis set (since this state has ionic character it is necessary to add sp-type diffuse functions to the basis set) and valence spaces which have been extended up to a 4 electron/10 π orbital CAS. The topology of all stationary points found (minimum, saddle points, etc.) has been assessed via vibrational frequency computations carried out at the same level of theory (see Ref. [27] for more details on $2A_1$ and $1B_2$ *s-cis* butadiene computations and Ref. [28] for *tZt* hexatriene $2A_1$ computations).

The photochemical paths leading to the final photoproducts are computed in two steps. In the first step we compute the MEP describing the S_1 relaxation from the Franck-Condon (FC) region of the systems under investigation. This MEP is unambiguously determined by using a new methodology [40,41] to locate the initial relaxation direction (IRD) from the starting point (i.e., the FC point). Briefly, an IRD corresponds to a local *steepest descent direction*, in *mass-weighted cartesians*, from a given starting point. The IRD is calculated by locating the energy minimum on a hyperspherical (i.e., $n-1$ dimensional) cross-section of the n dimensional potential energy surface centred on the starting point (n is the number of vibrational degrees of freedom of the molecule). The radius of this hypersphere is usually chosen to be small (typically ca. 0.25–1.5 a.u. in *mass-weighted cartesians*) in order to locate the steepest direction in the vicinity of the starting point (i.e., the hypersphere centre). The IRD is then defined as the vector joining the starting point (i.e., the centre of the hypersphere) to the energy minimum. Once the IRD has been determined, the MEP is computed as *the steepest descent line in mass-weighted cartesians* using the IRD vector to define the initial direction to follow. For example, as

[1] The DZ, DZ + d and DZ + spd basis sets used in this work correspond to the standard Gaussian 94 [35] basis sets (D95, D95* and D95 + *). See also Ref. [39].

we will discuss below, a twisted conical intersection structure (i.e., a S_1/S_0 real crossing point) has been located by simply following the resulting downhill S_1 PSB2 MEP until the S_1 and S_0 energies become degenerate. Also bifurcation points have been located on S_1 MEP (see Ref. [33]) through a series of hyperspherical optimizations at increasing radia: for smaller radia (from 0.25 to 0.75 a.u. *mass-weighted cartesians*) we found only one energy minimum per hypersphere, while two (PSB1) or three (PSB2) different hyperspherical minima were optimized for longer radia (1.0 and 1.5 a.u.). Thus, at the beginning, near the starting point, there is only one relaxation channel, that then splits originating distinct paths leading to chemically different structures. The same procedure has been used to locate bifurcations on S_0 MEP (see Section 3 for a detailed discussion of these points).

In the second step, we compute the MEP describing the S_0 relaxation processes from the S_1/S_0 conical intersection point (this is a highly unstable point, essentially a singularity, on the S_0 energy surface) determined in the first step. These MEP are determined with the same methodology choosing the intersection point as the starting point. There are different types of these IRD depending on the number of different S_0 relaxation paths connecting the intersection point to the final photoproducts S_0 energy minima.

3. Results and discussion

For each species investigated here, i.e., PSB1, PSB2 and the polyenes *s-cis* butadiene and *tZt* hexatriene, we have computed the MEP that connect the FC region to the photoproducts wells. A photochemical process can be separated in two equally important steps, which correspond to the evolution of the system in the excited state from the FC region to the conical intersection where decay occurs and to the evolution of the system from this conical intersection to the ground state with the formation of the various photoproducts. In Sections 3.1 and 3.2, we discuss first the MEP belonging to the excited states (see part (a) of Figs. 1–4) and subsequently those belonging to the ground states (see part (b) of Figs. 1–4).

3.1. Excited state MEP

In all cases investigated here we have found that the first excited state in the FC region is the spectroscopic–ionic state (HOMO → LUMO single excitation) in agreement with previous computational results [11–14,25]. While in the protonated Schiff bases the 1B ionic state remains always the first excited state, in the two polyenes the ionic $1B_2$ state crosses very early with the covalent $2A_1$ (double HOMO → LUMO excitation) state. Therefore, in the two protonated Schiff bases the relevant photochemical paths are located in the ionic 1B state while in the two analogous polyenes the photochemistry occurs on the covalent $2A_1$ state.

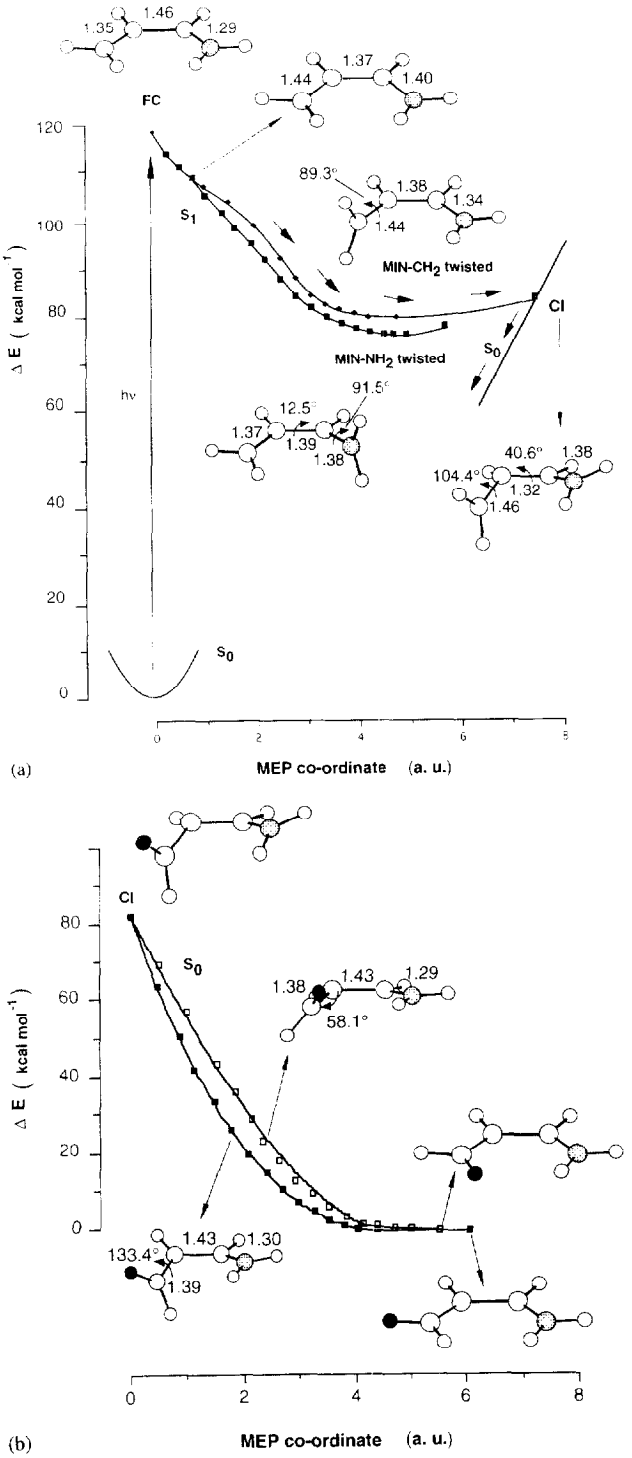

Fig. 1. PSB1 photochemistry (geometrical parameters in Å and degrees): (a) excited state MEP from the S_1 (1B) Frank-Condon (FC) structure to the two twisted minima (MIN-NH_2 twisted and MIN-CH_2 twisted) and S_1/S_0 conical intersection (CI); (b) S_0 relaxation MEP from the S_1/S_0 conical intersection point (CI) to the two possible photoproducts of isomerization. One terminal hydrogen atom in the structures has been highlighted to indicate the stereochemistry.

In the 1B state of PSB1 we have found two different MEP which, starting from the FC region, lead to two minima, one with the methylene group and the other with the imino group

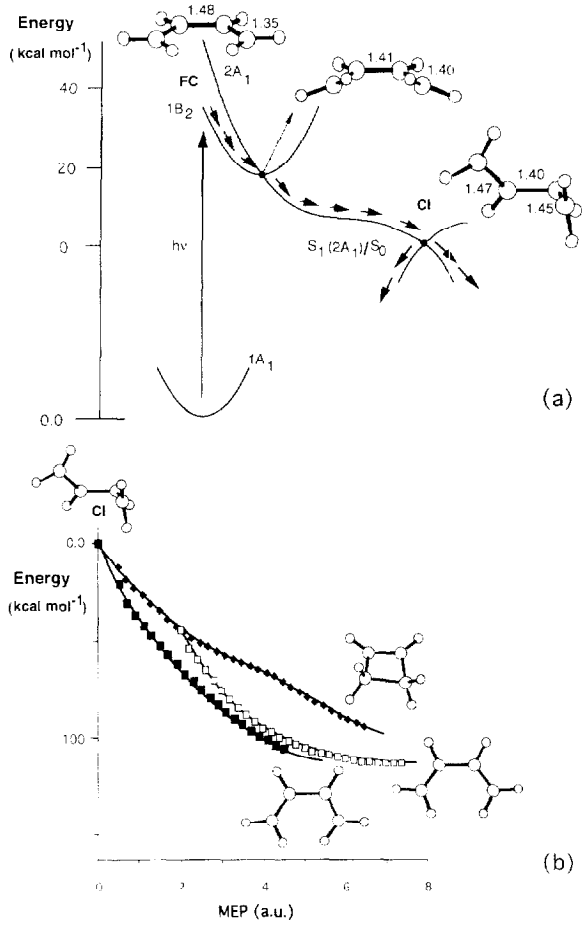

Fig. 2. *s-cis* Butadiene photochemistry (bond distances are in Å and angles of rotation in degrees): (a) computed MEP from the excited $1B_2$ Frank-Condon (FC) structure of *s-cis* butadiene to the S_1 ($2A_1$)/S_0 conical intersection (CI). Full lines and light lines represent the energy profile along the disrotatory and conrotatory MEP, respectively. The terminal hydrogen atoms in the structures have been highlighted to indicate the stereochemistry; (b) energy profiles along the computed MEP describing the relaxation from the S_1/S_0 conical intersection point (CI) to the *s-cis* butadiene photoproducts. The terminal hydrogen atoms in the structures have been highlighted to indicate the stereochemistry.

twisted of ~90° (see Fig. 1a). In the initial part of the two computed S_1 MEP, the motion is identical and dominated by stretching modes which result in an elongation of the two double bonds with a compression of the central single bond of the molecule: this process is associated with the change in bond order occurring in the excited state. The relaxation preserve the plane of symmetry of the molecule. After the initial relaxation the MEP bifurcates (see Section 2 on computational details) generating two distinct MEP leading to the two minima, so that the actual *cis*→*trans* isomerization motion is induced only after the in-plane bond stretching has been completed. In both minima, the S_0/S_1 energy gap is still large (~28 kcal/mol). Starting from these minima we have also searched for the existence of a conical intersection. We have found only one highly unsymmetric conical intersection in the region of the twisted methylene minimum, located only ~3 kcal/mol above it (see Fig. 1a for details on the energy profiles and the geometry of the structures discussed above).

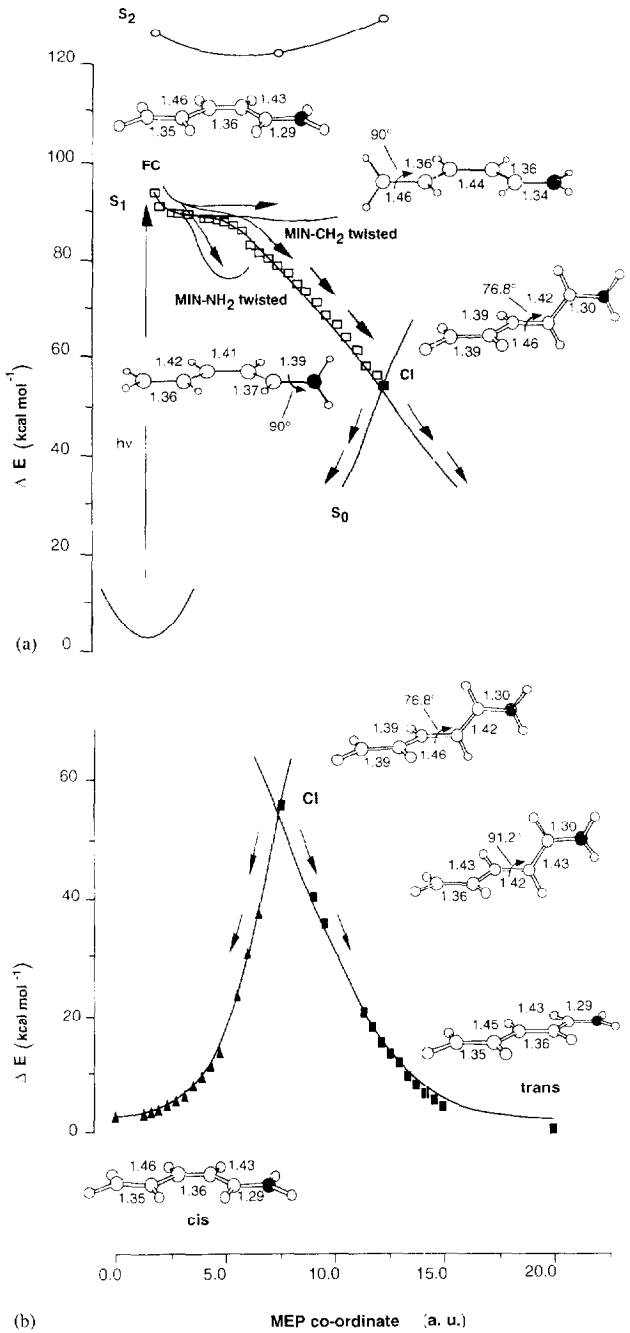

Fig. 3. PSB2 photochemistry (geometrical parameters in Å and degrees): (a) energy profile along the excited state MEP from the S_1 (1B) Frank-Condon (FC) structure to the S_1(1B)/S_0 conical intersection (CI). Also the two twisted minima (MIN-NH_2 twisted and MIN-CH_2 twisted) are represented; (b) S_0 relaxation MEP from the S_1/S_0 conical intersection point (CI) to the two possible photoproducts of isomerization: *tZt* 1-iminium-2,4-pentadiene (*cis*) and *tEt* 1-iminium-2,4-pentadiene (*trans*).

The photochemical behaviour of *s-cis* butadiene is significantly different (see Fig. 2a for comparison). In this case, after a very fast internal conversion (via a barrierless path involving a disrotatory motion of the terminal methylenes) between the spectroscopic $1B_2$ and the nearby dark $2A_1$ state, the photochemical path continues on the excited covalent state. Here there are two MEP, associated with disrotatory

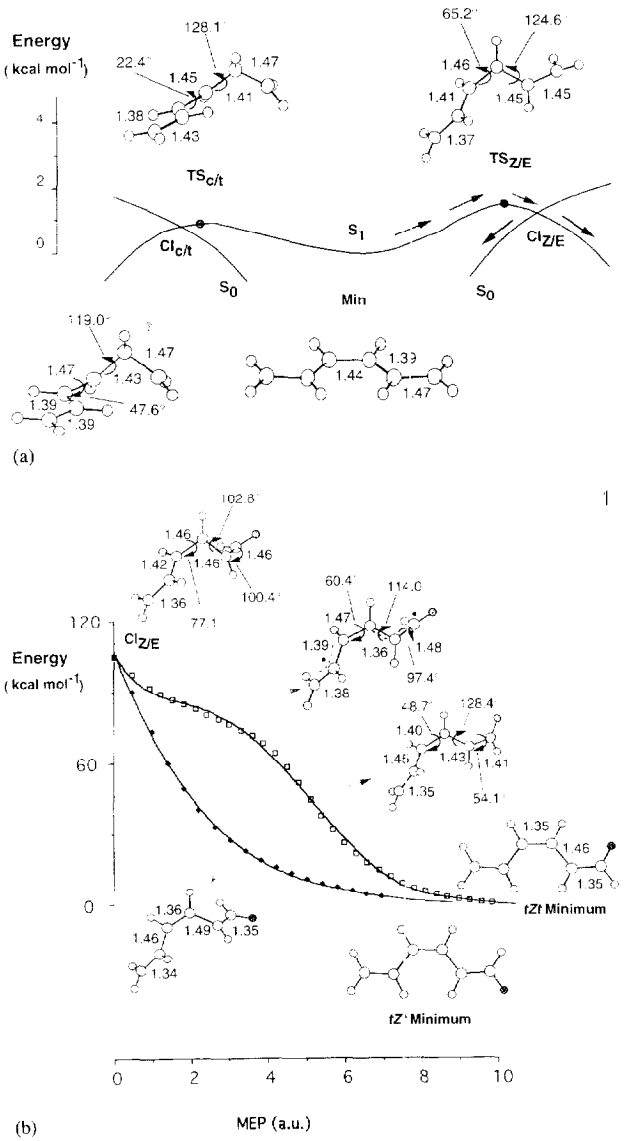

Fig. 4. *tZt* Hexatriene photochemistry (bond distances are in Å and angles of rotation in degrees): (a) computed reaction pathways from the S_1 ($2A_1$) minimum (Min) of *tZt* hexatriene to the two optimized transition states ($TS_{E/Z}$ and $TS_{c/t}$) leading to the two optimized S_1 ($2A_1$)/S_0 conical intersections ($CI_{E/Z}$ and $CI_{c/t}$); (b) energy profiles along the computed MEP describing the relaxation from the S_1/S_0 conical intersection *Z/E* ($CI_{Z/E}$) to the final photoproduct (the S_0 *tZt* hexatriene minimum *tZt* Minimum). The terminal hydrogen atom in the structures has been highlighted to indicate the stereochemistry.

and conrotatory motions of the methylenes. The disrotatory path is always energetically favoured and leads to a conical intersection without any barrier. These observations are consistent with spectroscopic studies which indicate that the ionic state is depopulated on a timescale of 10 fs and are in good agreement with the experimental evidence of lack of fluorescence [42] and disrotatory ring-closure (see Ref. [27] for a more detailed discussion). Because of the different electronic state involved in polyene and PSB photochemistry, the conical intersections in butadiene and in the corresponding PSB have different electronic structures. As already discussed, the conical intersection in butadiene (as well as in all other linear polyenes that we have studied [29,28,27,33,26]) corresponds to a tetraradicaloid species, while that in PSB1 originates from the intersection of a covalent and an ionic state. The covalent and ionic configurations differ by a one electron transfer (from the methylene to the imino group) between the two twisted fragments. Along the excited state MEP connecting the FC to the conical intersection region, the positive charge is progressively transferred from the *allyl-like*-CH–CH=NH_2 fragment to the CH_2– fragment. Thus at the conical intersection point the charge is completely localized on the *methylene* fragment (see Scheme 2).

For the longer Schiff base PSB2 [33] we have found three different barrierless MEP departing from a common initial excited state path which starts from the FC region (see Fig. 3a). Again, the common initial relaxation path preserve planarity and is dominated only by stretching modes without torsions: the central double bond of the molecule elongates in coincidence with the change in bond order occurring in the excited state of the molecule. After the initial in-plane stretching has been almost completed, (the hypothesis that the initial motion out of the FC region does not involve substantial torsion, has also been suggested by Delaney et al. [9] and Haran et al. [10] for bacteriorhodopsin), three different MEP are populated by different twists around the three double bonds. The two MEP associated with the twisting of the external double bonds lead to higher energy minima, while that associated with the central C=C double bond where isomerization occurs, leads to a lower energy conical intersection with a ~80° twist angle. This MEP is associated (as for the shorter Schiff base) with a progressive charge translocation from the *allyl-like* CH–CH=NH_2 to the *allyl* CH_2=CH–CH– twisted molecular fragments so that at the conical intersection one has the charge completely localized on the *allyl* CH_2=CH–CH– fragment. Going, through the

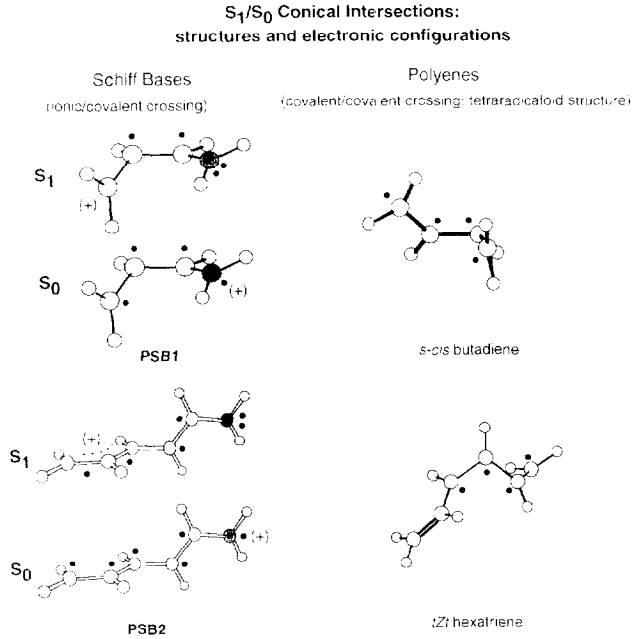

Scheme 2.

crossing, from the S_1 to the S_0 state a one electron transfer occurs between the two twisted fragments (from the imino to the polyenic one). Thus, the computed PSB conical intersections correspond to a type of twisted intramolecular charge transfer (TICT) state [38] (see Scheme 2).

For the analogous polyene *tZt* hexatriene we have found [28] two low energy competitive covalent excited $2A_1$ pathways (see Fig. 4a). A very fast internal conversion between the spectroscopic $1B_2$ state and the dark covalent $2A_1$ excited state occurs immediately after photoexcitation [42], so that the photochemistry of this system is driven by the potential energy surface of the $2A_1$ state. The computed reaction coordinates are associated with two possible *cis–trans* isomerization paths corresponding to a *c/t* and *Z/E* interconversion of the system. Like *s-cis* butadiene discussed above, the *cis–trans* isomerization paths do not terminate on the excited state potential energy surface. Rather, the *c/t* and *Z/E* pathways enter two different low lying conical intersections ($CI_{c/t}$ and $CI_{Z/E}$, in Fig. 4a) after overcoming very small energy barriers ($\sim$ 1 and 1.5 kcal/mol). These conical intersections are also essentially quasitetraradical species. Thus, while an excited state *tZt* hexatriene molecule can easily initiate a *cis–trans* isomerization process on $2A_1$, this process can be completed only on the ground state potential energy surface after passage through a crossing point (conical intersection) where a fast radiationless decay (an internal conversion) is possible. The conical intersections, which correspond to the final points of the computed excited state MEP (see Ref. [28] for a more detailed discussion), are located about one-third of the way along the ideal isomerization coordinate (i.e., the 180° rotation), so that a very low quantum yield of photoisomerization is expected (and indeed no *Z/E* relaxation path on S_0 was found, as we will see in Section 3.2). To localize possible double-bond photoisomerization processes, we have focused our attention on the *Z/E* isomerization path looking for the relaxation channels departing on S_0 from the nearby related conical intersection ($CI_{Z/E}$).

3.2. MEP for ground state relaxation

In this section, we discuss the ground state relaxation MEP that connects the conical intersections to photoproducts. These MEP are determined with the same methodology previously described, the only difference in this case being that the starting point is the conical intersection. In general, there may be several IRD (initial relaxation directions) associated with different S_0 relaxation paths connecting the conical intersection point to the final photoproducts S_0 energy minima.

We begin the discussion of the ground state relaxation MEP considering PSB1. In Fig. 1b, we illustrate the two different MEP, one associated with the rotation and the other with the reverse rotation of the twisted methylene group, leading to the two indistinguishable *cis–trans* double bond isomers (if we had different substituents at the rotating terminal carbon atom we would obtain two distinct isomers).

The situation is significantly different in *s-cis*-butadiene (see Fig. 2b) where we have found three channels [26]. One leads again to the double bond isomerization photoproduct, indistinguishable from the reactant because in this case we have identical terminal carbon atom substituents (two hydrogen atoms). The other to cyclobutene and the third one back to the reactant. The last two paths are generated through a bifurcation of an initial common relaxation valley (see Section 2 on computational details). These differences are determined from the different electronic nature and geometry of the starting conical intersection (as pointed out above). Thus, the recoupling of the quasitetraradical conical intersection electrons characterizes all the computed S_0 relaxation paths in *s-cis* butadiene and, as we will see, also in *tZt* hexatriene.

The ground state relaxation MEP of PSB2 are illustrated in Fig. 3b (see Ref. [33] for more details). Again, for this molecular system, we have found two distinct MEP, one leading back to the reactant (the *cis* isomer) and the other to the product of the photoisomerization (the *trans* isomer) through a rotation or a reverse rotation about the twisted central double bond which characterizes the ionic/covalent conical intersection. Thus the situation observed for this system is very similar to that discussed for the shorter protonated Schiff base PSB1.

For the analogous polyene *tZt* hexatriene, we have found again the MEP involving the recoupling of the electrons of the tetraradical-type conical intersection. In particular only two different MEP departing near the conical intersection point ($CI_{Z/E}$) have been located: one leads back to the *tZt* reactant while the other leads to a diradical transient species with an interesting recoupling scheme involving an inversion in the bond orders of the carbon atoms moiety. Thus, at the beginning of this second path, the recoupling of the four unpaired electrons is inverted with respect to the first MEP, which leads directly to the closed-shell *tZt* reactant, so generating an unstable bond-order inverted diradical. This diradical species subsequently evolves toward the more stable closed-shell *tZt* hexatriene, through the rotation of the twisted terminal methylene (which characterizes this highly unstable transient diradical, see the structures on Fig. 4b). Thus, at the end of this process, we obtain the external double-bond isomerization photoproduct, distinguishable from the reactant if we had different terminal carbon atom substituents. No central double-bond (*Z/E*) isomerization paths were found near the conical intersection; every attempt to localize this channel, also at distance of 5 $amu^{1/2}$ bohr from the conical intersection, leads back to the *tZt* reactant.

4. Conclusions

In this paper, we have reported the results of a study of the MEP obtained for the first excited state and for the ground state of two short-chain protonated Schiff bases, the protonated *s-cis* 1-iminium-2-propene (PSB1) and the protonated *tZt* 1-iminium-2,4-pentadiene (PSB2), and of the two anal-

ogous polyenes, *s-cis* butadiene and *tZt* hexatriene. Our results indicate that *the use of polyenes as models for the photochemical behaviour of PSB is not valid*. The photochemical behaviour of the PSB, which is always driven by the spectroscopic 1B ionic state, is significantly different from that of the analogous polyenes, driven by the covalent $2A_1$ state.

In the PSB studied, the lowest excited state is the spectroscopic ionic 1B state along all the computed MEP, while in the analogous polyenes the first excited state is initially again the spectroscopic ionic $1B_2$ state but becomes immediately, through a fast and efficient internal conversion, the covalent excited $2A_1$ state. The electronic and geometrical features of the computed MEP and conical intersections depend on the electronic structure of the excited states involved. The S_1/S_0 conical intersections in polyenes have a covalent tetraradicaloid character and are characterized by the development of a typical $-(CH)_3-$ 'kink' in the carbon moiety [29], while the S_1/S_0 conical intersections in the PSB have a twisted double-bond (the central double bond in PSB2 and the CH_2=CH– double bond in PSB1) and correspond to a TICT state.

Because of the difference in the electronic and geometrical features of the computed conical intersections in PSB and polyenes, the resulting relaxation paths in S_0 are quite different for the two systems. In polyenes, we found competitive relaxations corresponding to different recoupling schemes of the four unpaired electrons of the conical intersection (leading to external double bond isomerization products, reactant back-formation and ring-closure), while in the two PSB only very efficient *cis* → *trans* isomerization channels were localized. This may be one of the reason nature has chosen protonated Schiff bases as very efficient *cis–trans* isomerization switches.

References

[1] T. Yoshizawa, O. Kuwata, in: W.M. Horspool, P.-S. Song (Eds.), CRC Handbook of Organic Photochemistry and Photobiology, CRC Press, Boca Raton, FL (1995) 1493–1499.

[2] K.J. Rothschild, S. Sonar, in: W.M. Horspool, P.-S. Song (Eds.), CRC Handbook of Organic Photochemistry and Photobiology, CRC Press, Boca Raton, FL (1995) 1521–1544.

[3] R.W. Schoenlein, L.A. Peteanu, R.A. Mathies, C.V. Shank, Science 254 (1991) 412–415.

[4] Q. Wang, R.W. Schoenlein, L.A. Peteanu, R.A. Mathies, C.V. Shank, Science 266 (1994) 422–424.

[5] H. Kandori, H. Sasabe, K. Nakanishi, T. Yoshizawa, T. Mizukami, Y. Shichida, J. Am. Chem. Soc. 118 (1996) 1002–1005.

[6] H. Kandori, Y. Katsuta, M. Ito, H. Sasabe, J. Am. Chem. Soc. 117 (1995) 2669–2670.

[7] T. Mizukami, H. Kandori, Shichida, A.H. Chen, F. Derguini, C.G. Caldwell, C.Y. Bigge, K. Nakanishi, T. Yoshizawa, Proc. Natl. Acad. Sci. USA 90 (1993) 4072–4076.

[8] S.L. Logunov, L. Song, M. El-Sayed, J. Chem. Phys. 100 (1996) 18586–18591.

[9] J.K. Delaney, T.L. Brack, G.H. Atkinson, M. Ottolenghi, G. Steinberg, M. Sheves, Proc. Natl. Acad. Sci. USA 90 (1995) 2101–2105.

[10] G. Haran, K. Wynne, A. Xie, Q. He, M. Chance, R.M. Hochstasser, Chem. Phys. Lett. 261 (1996) 389–395.

[11] P. Du, E.R. Davidson, J. Phys. Chem. 94 (1990) 7013–7020.

[12] P. Du, C. Racine, E.R. Davidson, J. Phys. Chem. 94 (1990) 3944–3951.

[13] C.H. Martin, J. Phys. Chem. 100 (1996) 14310–14315.

[14] C.H. Martin, Chem. Phys. Lett. 257 (1996) 229–237.

[15] V. Bonacic-Koutecky, J. Köhler, J. Michl, Chem. Phys. Lett. 104 (1984) 440–443.

[16] V. Bonacic-Koutecky, K. Schöffel, J. Michl, Theor. Chim. Acta 72 (1987) 459–474.

[17] J.A. Dobado, M. Nonella, J. Phys. Chem. 100 (1996) 18282–18288.

[18] G.J. Dormans, G.C. Groenenboom, W.C.A. van Dorst, H.M. Buck, J. Am. Chem. Soc. 110 (1988) 1406–1415.

[19] R.M. Weiss, A. Warshel, J. Am. Chem. Soc. 101 (1979) 6131–6133.

[20] A. Warshel, N. Barboy, J. Am. Chem. Soc. 104 (1982) 1469–1476.

[21] R.R. Birge, L.M. Hubbard, J. Am. Chem. Soc. 102 (1980) 2195–2205.

[22] W. Humphrey, D. Xu, M. Sheves, K. Schulten, J. Phys. Chem. 99 (1995) 14549–14560.

[23] K. Andersson, P.A. Malmqvist, B.O. Roos, A.J. Sadlej, K. Wolinski, J. Phys. Chem. 94 (1990) 5483.

[24] K. Andersson, P.A. Malmqvist, B.O. Roos, J. Chem. Phys. 96 (1992) 1218.

[25] L. Serrano-Andrés, B.O. Roos, M. Merchán, Theor. Chim. Acta 87 (1994) 387.

[26] F. Bernardi, M. Olivucci, M.A. Robb, Chem. Soc. Rev. 25 (1996) 321.

[27] P. Celani, F. Bernardi, M.A. Robb, M. Olivucci, J. Chem. Phys. 102 (1995) 5733–5742.

[28] M. Olivucci, F. Bernardi, P. Celani, I. Ragazos, M.A. Robb, J. Am. Chem. Soc. 116 (1994) 1077–1085.

[29] P. Celani, M. Garavelli, S. Ottani, F. Bernardi, M.A. Robb, M. Olivucci, J. Am. Chem. Soc. 117 (1995) 11584–11585.

[30] L.D. Landau, Phys. Z. Sowjetunion 2 (1932) 46.

[31] C. Zener, Proc. R. Soc. London, Ser. A 137 (1932) 696.

[32] J. Michl, V. Bonacic-Koutecky, Electronic Aspects of Organic Photochemistry, Wiley, New York, 1990.

[33] M. Garavelli, P. Celani, F. Bernardi, M.A. Robb, M. Olivucci, J. Am. Chem. Soc., 119 (1997) 6891–6901.

[34] B.O. Roos, Adv. Chem. Phys. 69 (1987) 399–446.

[35] The MC-SCF programme we used is implemented in Gaussian 94, Revision B.2, M.J. Frisch, G.W. Trucks, H.B. Schlegel, P.M.W. Gill, B.G. Johnson, M.A. Robb, J.R. Cheeseman, T. Keith, G.A. Petersson, J.A. Montgomery, K. Raghavachari, M.A. Al-Laham, V.G. Zakrzewski, J.V. Ortiz, J.B. Foresman, C.Y. Peng, P.Y. Ayala, W. Chen, M.W. Wong, J.L. Andres, E.S. Replogle, R. Gomperts, R.L. Martin, D.J. Fox, J.S. Binkley, D.J. Defrees, J. Baker, J.P. Stewart, M. Head-Gordon, C. Gonzalez, J.A. Pople, Gaussian, Pittsburgh, PA, (1995).

[36] K. Andersson, P.A. Malmqvist, B.O. Ross, J. Chem. Phys. 96 (1992) 1218.

[37] MOLCAS, Version 3, K. Andersson, M.R.A. Blomberg, M. Fülscher, V. Kellö, R. Lindh, P.-A. Malmqvist, J. Noga, J. Olsen, B.O. Roos, A.J. Sadlej, P.E.M. Siegbahn, M.. Urban, P.O. Widmark, University of Lund, Sweden (1994).

[38] G.J. Kavarnos, Fundamentals of Photoinduced Electron Transfer, VCH, New York, 1993.

[39] T.H. Dunning, P.J. Hay, Methods of Modern Theoretical Chemistry, in: H.F. Shaefer (Ed.), Plenum, New York, Vol. 3 (1977) pp. 1–27.

[40] P. Celani, M.A. Robb, M. Garavelli, F. Bernardi, M. Olivucci, Chem. Phys. Lett. 243 (1995) 1–8.

[41] M. Garavelli, P. Celani, M. Fato, M.J. Bearpark, B.R. Smith, M. Olivucci, M.A. Robb, J. Phys. Chem. A 101 (1997) 2023.

[42] M.O. Trulson, R.A. Mathies, J. Phys. Chem. 94 (1990) 5741.